Friction-Induced Transformation from Graphite Dispersed in Esterified Bio-Oil to Graphene

Xu, Yufu; Geng, Jian; Zheng, Xiaojing; Dearn, Karl; Hu, Xianguo

DOI:
10.1007/s11249-016-0708-5

Friction-Induced Transformation from Graphite Dispersed in Esterified Bio-oil to Graphene

Yufu Xu[a*], Jian Geng[a], Xiaojing Zheng[b], Karl D. Dearn[c], Xianguo Hu[a]

a. Institute of Tribology, School of Mechanical and Automotive Engineering, Hefei University of Technology, Hefei 230009, China

b. School of Arts and media, Hefei Normal University, Hefei 230601,China

c. School of Mechanical Engineering, University of Birmingham, Edgbaston, Birmingham B152TT, United Kingdom

Abstract: Fabricating high-quality graphene with simple methods has aroused considerable interests in recent years. In this paper, graphite was dispersed in esterified bio-oil (EBO) as a lubricant for steel/gray cast iron friction pairs, and the shear-induced transformation from graphite to graphene was observed. The tribological behavior during this process, including the influence of the normal load and sliding velocity, were investigated. The products formed after sliding were confirmed by laser particle size analyzer, Raman spectroscopy and scanning electron microscopy (SEM). The micro-topographies and elemental content of the worn surfaces were measured by SEM and energy-dispersive X-ray spectrometry (EDX). The results showed that friction induces exfoliation accounting for the transformation from graphite into graphene, and the frictional conditions have great influence on the products. It was also found that high load and low sliding velocity facilitate the formation of high-quality single-layer graphene during the sliding process, and high load and low sliding velocity also contributed to obtaining excellent tribological

* Corresponding author. Tel.: +86 551 62901359; fax: +86 551 62901359.

E-mail: xuyufu@hfut.edu.cn

performance for friction pairs. Friction-induced transformation shows a new potential for graphene preparation.

Keywords: Friction-induced transformation; Graphite; Graphene; Esterified Bio-oil

1. Introduction

Graphene, a two dimensional layer carbon with sp^2-bonded carbon, is of considerable interest [1-6] because of its excellent conductivity, high mechanical strength and controllable permittivity, and has many potential applications to energy storage [7], micro-electronics [8], lubrication [9], etc [10]. Many preparation methods have been proposed, including mechanical exfoliation [11], epitaxial growth [12], chemical vapor deposition [13], and reduction of graphene oxide (GO) [14]. Although there has been much progresses in fabricating graphene, the cost and quality of the graphene [15, 16] still remains an issue.

Graphite has been used as lubricants additives for more than one hundred years [17]. In the past, most attentions have been paid on the macroscopic lubricating applications[18-20]. Recently, the friction and wear mechanisms of graphite have been studied and proposed that the interlamellar binding forces of graphite were slight and made graphite slippery [21], which resulted in a low friction coefficient and low wear of friction pairs. Unfortunately, few literatures have systematically investigated the debris of the graphite after sliding, though the debris could also influent the tribological behavior. Theoretically, graphite could exfoliate its layers during sliding [22] and form multi-layer carbon, and also could form single-layer graphene under certain condition. Additionally, it has been proved that graphite as lubricating additives is environmental dependent [23]. Therefore, the dispersed media are very important for graphite during sliding.

To date, a relatively small amount of work has explored friction-induced products formation

from graphite dispersed in a medium. In this work, we chose esterified bio-oil (EBO) as a medium for graphite. EBO, synthesized by converting the acids to esters in the bio-oil has shown good potential for reducing the corrosive behavior of the crude bio-oils [24-26]. However, the lubricity of EBO still needs to be further improved to be used as a fuel. In our previous work, we found that MoS_2 and graphene had a very good synergetic lubricating effect when dispersed in EBO and could enhance its lubricity significantly [26]. Therefore, using graphite as lubricating additives for EBO not only enables it possible to improve the friction and wear behavior of EBO, but also makes us to know more about the friction-induced exfoliation of graphite. The tribological conditions, including the normal load and sliding speed here investigated to explore their effects during the sliding. The corresponding tribological mechanisms were also explored.

2. Experimental details

2.1 Materials

Flake graphite (purity 99%) was purchased from Qingdao Haida Graphite Co. Ltd., (Qingdao, China), and was used directly, without further purification. Its size ranges from 124 to 1408 μm and mean particle size is ~500μm (**Fig. 1a**). A typical micrograph edges of the graphite plates is shown in the inset of **Fig. 1a**, indicating a multiple-layer structure of carbon. The Raman spectrum (**Fig. 1b)** shows the D (~1354 cm^{-1}), G (~1580 cm^{-1}) and 2D (~2713 cm^{-1}) bands of graphite. The D peak results from the breathing mode of the sp^2-C atoms, which is induced by structural disorder defects [27]. The ratio intensity, $I_D/I_G = 0.154$, suggesting a low degree of graphic disorder of the graphite.

EBO was fabricated from crude *Spirulina* algae bio-oil via catalytic esterification [24]. The main components were oxygen-containing organics. More details of its chemical components and physical properties can be found in our previous work [24].

2.2 Tribological tests

The apparatus has used to measure friction and wear is shown in **Fig. 2.** The cylinder upper friction pair friction pair was made from AISI 304 stainless steel with the outside diameter of 32mm and inside diameter of 22mm. Six grooves distributed symmetrically on the cylinder. The lower friction pair was a round disk with diameter of 40mm and was made from gray cast iron HT 150 (ASTM-A48 No. 25A). The surface roughness Ra of the friction interface of cylinder and disk were 0.58 and 0.61 μm, respectively.

In a typical test, 1.0 g graphite was dissolved in 50 mL of EBO. After ultrasonic dispersion for 20 min, the suspension was placed in the oil reservoir of the tribometer. The samples were tested under loads of 100, 150, and 200N, and using sliding speeds of 0.1, 0.2, and 0.3 m/s. Each test was repeated twice. The wear rate was calculated from the difference between the weight of lower friction pair per sliding distance before and after sliding.

After the friction experiments, the liquid products were analyzed with Agilent Cary 5000 UV–Vis–NIR spectrophotometer over the range 200 to 1000 nm. The liquid was filtered and the solid power and the friction pairs were washed with acetone, and dried at 40°C in vacuum drying oven.

2.3 Characterization

The diameter of the solid particles before and after sliding were tested using a Malvern MS-2000 laser particle-size analyzer. Raman spectra of the solid particles before and after sliding were measured using a Horiba Jobin Yvon LabRam HR Evolution Raman spectrometer using a emitting 532 nm radiation. The microstructure of the solid particles and the rubbed surfaces were analyzed with an JEOL JSM-6490LV scanning electron microscopy (SEM), and analyzed using

energy dispersive X-ray spectrometry (EDX).

3. Results and discussion

3.1 Influence of load

The successful fabricating of graphene is confirmed by UV–vis spectroscopy (**Fig. 3**). From the figure, it can be seen that the absorption intensity increased after sliding. This suggests that more graphite sheets are present in the solvent, due to exfoliation of graphite during sliding [28]. Furthermore, graphite displays a peak maximum at ~225 nm with a shoulder at ~237 nm, while after sliding peaks redshifts slightly to 227 and 253 nm, respectively. This may be caused by the formation of auxochromic groups such as –OH owing to the friction oxidation [29]; and also indicated that the electronic conjugation of graphene sheets is restored after the tribo-reaction [30].

Fig.4 shows the particle size distribution and Raman spectra of the lubricant graphite sliding under different loads. As shown in Fig.4a, the particle size of the products decreased with increasing load, indicating higher load contributed to the exfoliation of graphite. Raman spectra are considered as a very effective technology to investigate the layer of the graphene [31]. It can be seen from Fig. 4b that the D, G and 2D bands of the products were detected, and the I_D/I_G ratio decreased with increasing load, suggesting higher loads helped to reduce the defects of the graphene. Meanwhile, all the 2D peaks (inset of Fig.4b) is obviously different from the graphite in Fig.1b and can be resolved into four components, $2D_{1B}$, $2D_{1A}$, $2D_{2A}$, $2D_{2B}$; two of them are higher than the other two; the intensity of 2D band is close to that of G band, indicating that the main products are bilayer graphene [32].

Micrographs of the particles in the lubricant after sliding under different loads are shown in **Fig. 5.** There is a clear exfoliation of the graphene sheets seen in Fig. 5a. The graphene sheets in Fig.

5a, b and c hold their original laminated structure from graphite, with diameters between ~4 to ~20 μm, which are similar with the results reported by Lin et al [33]. In addition, with an increase in load, the graphene had much smoother surface and smaller particle size. These trends were in accord with the particle size distribution in Fig.4a. The detailed diameters in Fig. 5 are different from those in Fig. 4a because of the different analysis method. Only several particles can be observed in SEM images, while the total statistical results can be obtained by using laser particle-size analyzer.

Fig. 6 presents the friction coefficient and wear rate of the stationary sample lubricated with EBO and graphite dispersed in EBO under different loads. Shown in Fig.6a is the friction coefficient of EBO with graphite (0.083), which was much lower than that of pure EBO (0.116) both under load of 100N, and it decreased by more than 28%, indicating that graphite had a beneficial lubricating role. Furthermore, the EBO with graphite had a shorter run-in period than pure EBO. This may be due to the exfoliation of graphite making small graphene sheets fill in the furrows and quickly forming a tribo-film on the rubbing surfaces [34]. The run-in period also decreased with increasing load. In addition, the steady stage friction coefficient for EBO with graphite decreased from 0.076 to 0.059 with an increase in load from 100 to 200N. This may because higher load leads to a larger plastic deformation of the stationary sample, increasing real contact area, which makes more graphene sheets fill in or adsorb on the rubbing surfaces, and then decreases the contact stress of the friction pairs [35], finally, the coefficient of friction decreases.

From the Fig.6 b, it can be seen that the wear rate of the stationary sample lubricated by EBO with graphite decreased by more than 44%, comparing to that lubricated by pure EBO. The wear rate almost linearly decreased from 0.0068 to 0.0037 mg/m with an increase in load from 100 to 200 N when lubricated with EBO with graphite. Moreover, another result that higher load made for

less wear might because under higher load, more graphene sheets remained on the rubbing surfaces, alleviating the material remove rate.

Fig. 7 shows the micrographs of worn surfaces of the stationary sample that had been lubricated with EBO and EBO with graphite under different loads. The surfaces lubricated by EBO alone showed clear delamination wear [36]. While with adding of graphite, wear was reduced and the surface exhibited some spalling pits on the surfaces under a load of 100N. Adhesive material and furrows occurred when the load has increased to 150N. The surfaces became much smoother with only some light furrows under a load of 200 N, indicating a mild wear. According to these micrographs and tribological data above, these four wear types of Fig.7 may belong to delamination wear, spalling wear, adhesive wear and mild wear, respectively. That is, the graphite as EBO additives could prevent the rubbed surfaces from delamination and further reduce wear under higher loads. Higher loads, much smoother of worn surfaces, which agreed very well with less wear rate under higher loads in Fig. 6.

Fig.8 displays the EDX results of the worn surfaces of the stationary sample lubricated with EBO and EBO with graphite under different loads. It can be seen that, for pure EBO lubrication (Fig.8a), the carbon and oxygen on the worn surfaces could come from EBO decomposition [24], while the chromium might originate from the transfer from the AISI 304 stainless steel counterface [37]. The rubbed surfaces lubricated with EBO with graphite (Fig.8b) had higher contents of carbon and oxygen than that lubricated by the pure EBO (Fig.8a), indicating that during the frictional process, the graphite can be exfoliated into graphene, and then some of graphene can be reacted onto the worn surfaces to form the complex tribo-film [38]. Furthermore, this tribo-reaction increased at higher loads (Fig8b-d) since large amounts of carbon were detected. That is, friction-induced exfoliation makes graphite transform into graphene, and then adsorbed or reacted

on the rubbing surfaces. Moreover, higher loads makes more graphene and thicker tribo-film, decreasing the friction coefficient and wear rate and also confirming the inference for the results in Fig. 6. Therefore, in the following section, a higher load of 250N was chosen for investigating the influence of sliding speed.

3.2 Influence of sliding speed

Fig.9 shows the UV–vis spectra of graphite dispersed in EBO before and after sliding at different speeds. After friction, both of the peak maximum and shoulder red shifted to higher wavelength, 232 and 253nm, respectively, indicating that the electronic conjugation within the graphene increased after friction [30]. Moreover, the absorbance increased with increasing sliding speed, indicating that higher sliding speed is helpful for formation of more auxochromic groups including hydroxyl groups due to the enhance of the tribo-oxidation reaction [39].

Fig. 10 displays the particle size distribution and Raman spectra of the graphite particles in the liquid after sliding at different sliding speed. As can be seen from the Fig. 10a, the particle size decreased and distribution became narrower with an increase in sliding speed. This may because higher speeds are easy to exfoliate the graphite into smaller pieces. From Fig.10b, it can be seen that the typical single-layer graphene can be obtained at speed of 0.1m/s, since that the intensity of single 2D peak is two times of that of G peak [32]. Main components of the products are bilayer graphene and few-layer graphene with some graphite at speed of 0.2 and 0.3 m/s, respectively, because the intensity of 2D band is ~0.9 and ~0.6 times of G band [40] at speed of 0.2 and 0.3 m/s. The D band peaks disappeared at the sliding velocity of 0.1 and 0.2m/s, but occurred again at 0.3m/s, indicating high-quality single-layer graphene could be obtained [32] at low sliding speed of 0.1m/s, but the defect increased on the carbon layer of the products at higher speed.

Fig. 11 displays the micrographs of the particles in the fluid after sliding at different sliding speeds. As shown, large slice structures with wrinkles of the graphene remained at low sliding speeds, while higher sliding speed led to exfoliate the products into small pieces. These image results agree with the Raman spectra in Fig. 10b.

The friction and wear behavior of the contacts lubricated with graphite dispersed in EBO at different sliding speeds are shown in **Fig. 12.** Fig. 12a shows that, at the run-in and initial stage, with an increase in sliding speed, the friction coefficient decreased accordingly. However, at follow-up stage, the friction coefficient under high sliding speed (0.3m/s) is higher than that under low sliding speed (0.1m/s). This might because high sliding speed contributed to the formation of the tribo-film at initial stage, but also will destroy the tribo-film by lasting friction at follow-up stage [35]. Fig. 12b shows that the wear rate increased slightly with an increase of sliding speed. This can be explained by the fact that at high sliding speed, the graphite and graphene remain on the rubbing surfaces for shorter time than those under lower sliding speed [26], and also under the high sliding speed the friction pairs will much easier to destroy the tribo-film on the rubbing surfaces on the counterparts.

Fig. 13 shows micrographs of worn surfaces of stationary sample lubricated with graphite dispersed in EBO at different sliding speeds. It can be noted that there were some thin and dense furrows on the worn surfaces at low speed (Fig.13a), suggesting it had only slight wear. The surface roughness increased and wear furrows became wider with an increase in sliding speed (Fig.13b, c), indicating the wear types belong to a mild wear and severe wear, respectively [41].

Fig. 14 shows the EDX results of the worn surfaces of stationary sample lubricated with graphite dispersed in EBO at different sliding speeds. As shown in the figures, the relative contents of carbon and oxygen decreased with an increase in sliding speed, indicating tribo-film became

thinner under high sliding speed. The element chromium resulted from the upper friction pair owing to the material transfer during sliding [42]. The element Fe from substrate can also be detected. Besides, the element silicon was found on the worn surfaces at high sliding speed, which came from inside of the substrate of gray cast iron, confirming the high sliding speed may destroy the tribo-film and is harmful to the formation of single-layer graphene.

3.3 Tribological mechanisms

According to all the experimental results above, an schematic explanation of the tribological mechanisms is shown in **Fig. 15.** As shown, under sliding conditions, the suspended graphite was transformed into multi-/single- layer graphene, and formed a thin tribo-film on the rubbed surfaces, which decreases the friction and wear. With an increase in load, the shear effects enhanced and smaller graphene particles size of the graphene were obtained, which led to a thick tribo-film on the surfaces, resulting in a lower friction and wear. When the sliding speed changed, the products altered accordingly. On one hand, at high speed, small graphene particle were formed. At initial stage, it was easy to form a thick tribo-film on the surface, resulting in a low friction coefficient at this stage. However, during sliding, the tribo-film was destroyed at higher sliding speeds, and then the friction and wear of the samples increased. On the other hand, at lower speeds, although the tribo-film was not very thick, but it maintained on the surfaces for a longer time than those under high speed friction, which resulted in a lower friction and wear at the end of the friction.

4. Conclusions

Graphite was dispersed in EBO and played a beneficial lubricating role between a upper rotational and lower stationary steel/gray cast iron pairs. The products were analyzed and the

tribological behavior during this process was recorded. The friction and wear mechanisms were investigated. Several conclusions can be drawn from this work:

1. Friction-induced transformation is an effective method to fabricate graphene from graphite. High load and low sliding velocity contribute to the formation of high-quality single-layer graphene during the sliding process.
2. Exfoliation induced by sliding makes graphite transform into graphene, and then it adsorbed or reacted on the rubbing surfaces to prevent the material from severe wear. In addition, higher loads makes more graphene and thicker tribo-film, decreasing the friction coefficient and wear rate. The wear types of the friction pairs lubricated by EBO with graphite are ascribed to spalling wear, adhesive wear and mild wear, respectively, with the increasing loads.
3. The higher sliding speed helps to form a thicker tribo-film composed of graphene and other components on the rubbing surfaces at initial stage, which results in a low friction and wear, but at the follow-up stage, the tribo-film is more easier to be destroyed at higher sliding speeds, and then the friction and wear of the samples increased. The wear types change from slight wear, to mild wear and to severe wear with an increase in sliding velocity.

Acknowledgments

This work is supported by the National Natural Science Foundation of China (Grant No. 51405124), China Postdoctoral Science Foundation (Grant No. 2015T80648) and the Anhui Provincial Natural Science Foundation (Grant No. 1408085ME82).

References

[1] Zhang, Y., Tan, Y.-W., Stormer, H.L., Kim, P.: Experimental observation of the quantum Hall effect and Berry's phase in graphene. Nature **438**, 201-204 (2005)

[2] Li, X., Cai, W., An, J., Kim, S., Nah, J., Yang, D., Piner, R., Velamakanni, A., Jung, I., Tutuc, E.: Large-area synthesis of high-quality and uniform graphene films on copper foils. Science **324**, 1312-1314 (2009)

[3] Kostarelos, K., Novoselov, K.S.: Exploring the interface of graphene and biology. Science **344**, 261-263 (2014)

[4] Bonaccorso, F., Colombo, L., Yu, G., Stoller, M., Tozzini, V., Ferrari, A.C., Ruoff, R.S., Pellegrini, V.: Graphene, related two-dimensional crystals, and hybrid systems for energy conversion and storage. Science **347**, 1246501 (2015)

[5] Le, T.X.H., Bechelany, M., Lacour, S., Oturan, N., Oturan, M.A., Cretin, M.: High removal efficiency of dye pollutants by electron-Fenton process using a graphene based cathode. Carbon **94**, 1003-1011 (2015)

[6] Novoselov, K.S., Geim, A.K., Morozov, S., Jiang, D., Zhang, Y., Dubonos, S.a., Grigorieva, I., Firsov, A.: Electric field effect in atomically thin carbon films. Science **306**, 666-669 (2004)

[7] Raccichini, R., Varzi, A., Passerini, S., Scrosati, B.: The role of graphene for electrochemical energy storage. Nature Mater. **14**, 271-279 (2015)

[8] Wu, K.-H., Cheng, H.-H., Mohammad, A.A., Blakey, I., Jack, K., Gentle, I.R., Wang, D.-W.: Electron-beam writing of deoxygenated micro-patterns on graphene oxide film. Carbon **95**, 738-745 (2015)

[9] Yao, J., Shi, X., Zhai, W., Ibrahim, A.M.M., Xu, Z., Chen, L., Zhu, Q., Xiao, Y., Zhang, Q., Wang, Z.: The enhanced tribological properties of NiAl intermetallics: Combined lubrication of multilayer graphene and WS_2. Tribol. Lett. **56**, 573-582 (2014)

[10] Kay, L., Porter, A.L., Youtie, J., Rafols, I., Newman, N.: Mapping graphene science and development: Focused research with multiple application areas. Bulletin of the American Society for Information Science and Technology **41**, 22-25 (2015)

[11] Yi, M., Shen, Z.: A review on mechanical exfoliation for the scalable production of graphene. Journal of Materials Chemistry A **3**, 11700-11715 (2015)

[12] Tetlow, H., De Boer, J.P., Ford, I., Vvedensky, D., Coraux, J., Kantorovich, L.: Growth of epitaxial graphene: Theory and experiment. Physics Reports **542**, 195-295 (2014)

[13] Strudwick, A.J., Weber, N.E., Schwab, M.G., Kettner, M., Weitz, R.T., Wünsch, J.R., Müllen, K., Sachdev, H.: Chemical vapor deposition of high quality graphene films from carbon dioxide atmospheres. ACS nano **9**, 31-42 (2014)

[14] Chua, C.K., Pumera, M.: Chemical reduction of graphene oxide: a synthetic chemistry viewpoint. Chem. Soc. Rev. **43**, 291-312 (2014)

[15] Novoselov, K.S., Fal, V., Colombo, L., Gellert, P., Schwab, M., Kim, K.: A roadmap for graphene. Nature **490**, 192-200 (2012)

[16] Kuila, T., Bose, S., Hong, C.E., Uddin, M.E., Khanra, P., Kim, N.H., Lee, J.H.: Preparation of functionalized graphene/linear low density polyethylene composites by a solution mixing method. Carbon **49**, 1033-1037 (2011)

[17] Barham, G.: Good and Bad Lubricants. Journal of the American Society for Naval Engineers **27**, 694-697 (1915)

[18] Shaji, S., Radhakrishnan, V.: Analysis of process parameters in surface grinding with graphite as lubricant based on the Taguchi method. J. Mater. Process. Technol. **141**, 51-59 (2003)

[19] Alberts, M., Kalaitzidou, K., Melkote, S.: An investigation of graphite nanoplatelets as lubricant in grinding. International Journal of Machine Tools and Manufacture **49**, 966-970 (2009)

[20] Suresh Kumar Reddy, N., Venkateswara Rao, P.: Performance improvement of end milling using graphite as a solid lubricant. Mater. Manuf. Process. **20**, 673-686 (2005)

[21] Kumar, N., Dash, S., Tyagi, A.K., Raj, B.: Super low to high friction of turbostratic graphite under various atmospheric test conditions. Tribol. Int. **44**, 1969-1978 (2011)

[22] Toyoda, M., Inagaki, M.: Heavy oil sorption using exfoliated graphite: New application of exfoliated graphite to protect heavy oil pollution. Carbon **38**, 199-210 (2000)

[23] Marks, N.: Generalizing the environment-dependent interaction potential for carbon. Phys. Rev. B **63**, 035401 (2000)

[24] Xu, Y., Zheng, X., Hu, X., Dearn, K.D., Xu, H.: Effect of catalytic esterification on the friction and wear performance of bio-oil. Wear **311**, 93-100 (2014)

[25] Xu, Y., Hu, X., Yuan, K., Zhu, G., Wang, W.: Friction and wear behaviors of catalytic methylesterified bio-oil. Tribol. Int. **71**, 168-174 (2014)

[26] Xu, Y., Peng, Y., Dearn, K.D., Zheng, X., Yao, L., Hu, X.: Synergistic lubricating behaviors of graphene and MoS_2 dispersed in esterified bio-oil for steel/steel contact. Wear **342**, 297-309 (2015)

[27] Schmucker, S.W., Cress, C.D., Culbertson, J.C., Beeman, J.W., Dubon, O.D., Robinson, J.T.: Raman signature of defected twisted bilayer graphene. Carbon **93**, 250-257 (2015)

[28] Liang, S., Shen, Z., Yi, M., Liu, L., Zhang, X., Ma, S.: In-situ exfoliated graphene for high-performance water-based lubricants. Carbon **96**, 1181-1190 (2016)

[29] Han, H., Gao, Y., Zhang, Y., Du, S., Liu, H.: Effect of magnetic field distribution of friction surface on friction and wear properties of 45 steel in DC magnetic field. Wear **328**, 422-435 (2015)

[30] Li, D., Muller, M.B., Gilje, S., Kaner, R.B., Wallace, G.G.: Processable aqueous dispersions of graphene nanosheets. Nat Nano **3**, 101-105 (2008)

[31] Ferrari, A.C., Meyer, J.C., Scardaci, V., Casiraghi, C., Lazzeri, M., Mauri, F., Piscanec, S.,

Jiang, D., Novoselov, K.S., Roth, S., Geim, A.K.: Raman spectrum of graphene and graphene layers. Phys. Rev. Lett. **97**, 187401 (2006)

[32] Ferrari, A.C.: Raman spectroscopy of graphene and graphite: disorder, electron–phonon coupling, doping and nonadiabatic effects. Solid State Commun. **143**, 47-57 (2007)

[33] Lin, J., Wang, L., Chen, G.: Modification of graphene platelets and their tribological properties as a lubricant additive. Tribol. Lett. **41**, 209-215 (2011)

[34] Chen, B., Bi, Q., Yang, J., Xia, Y., Hao, J.: Tribological properties of solid lubricants (graphite, h-BN) for Cu-based P/M friction composites. Tribol. Int. **41**, 1145-1152 (2008)

[35] Xu, Y.F., Zheng, X.J., Yin, Y.G., Huang, J., Hu, X.G.: Comparison and analysis of the influence of test conditions on the tribological properties of emulsified bio-oil. Tribol. Lett. **55**, 543-552 (2014)

[36] Gong, T., Yao, P., Xiao, Y., Fan, K., Tan, H., Zhang, Z., Zhao, L., Zhou, H., Deng, M.: Wear map for a copper-based friction clutch material under oil lubrication. Wear **328**, 270-276 (2015)

[37] Muthuraja, A., Senthilvelan, S.: Adhesive wear performance of tungsten carbide based solid lubricant material. International Journal of Refractory Metals and Hard Materials **52**, 235-244 (2015)

[38] Major, L., Janusz, M., Kot, M., Lackner, J., Major, B.: Development and complex characterization of bio-tribological Cr/CrN+ aC: H (doped Cr) nano-multilayer protective coatings for carbon–fiber-composite materials. RSC Advances **5**, 9405-9415 (2015)

[39] Li, X., Zhou, Y., Ji, X., Li, Y., Wang, S.: Effects of sliding velocity on tribo-oxides and wear behavior of Ti–6Al–4V alloy. Tribol. Int. **91**, 228–234 (2015)

[40] Allen, M.J., Tung, V.C., Kaner, R.B.: Honeycomb carbon: a review of graphene. Chem. Rev. **110**, 132-145 (2009)

[41] Wang, L., Zhang, Q., Li, X., Cui, X., Wang, S.: Severe-to-mild wear transition of titanium alloys as a function of temperature. Tribol. Lett. **53**, 511-520 (2014)

[42] Karlsson, P., Gåård, A., Krakhmalev, P.: Influence of tool steel microstructure on friction and initial material transfer. Wear **319**, 12-18 (2014)

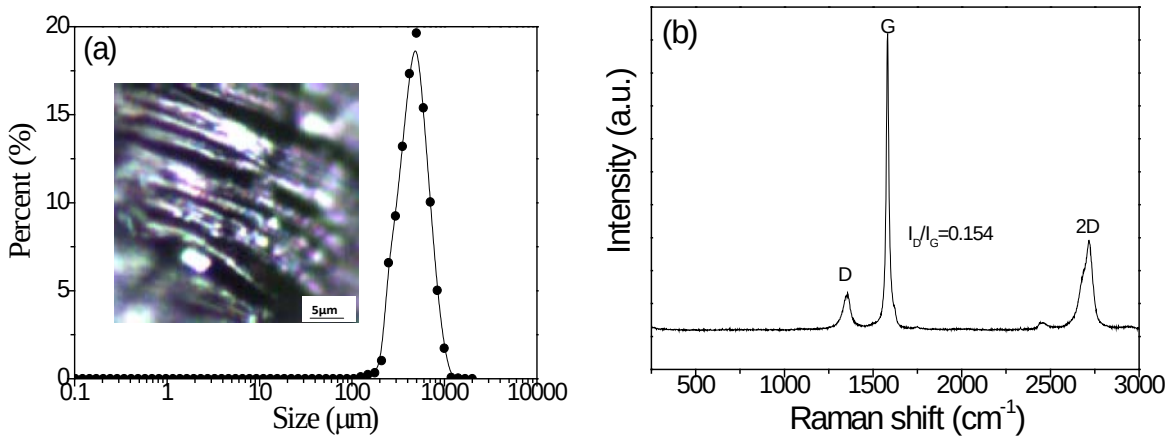

Fig.1 (a) Particle size distribution, micrograph (inset) and (b) Raman spectrum of graphite

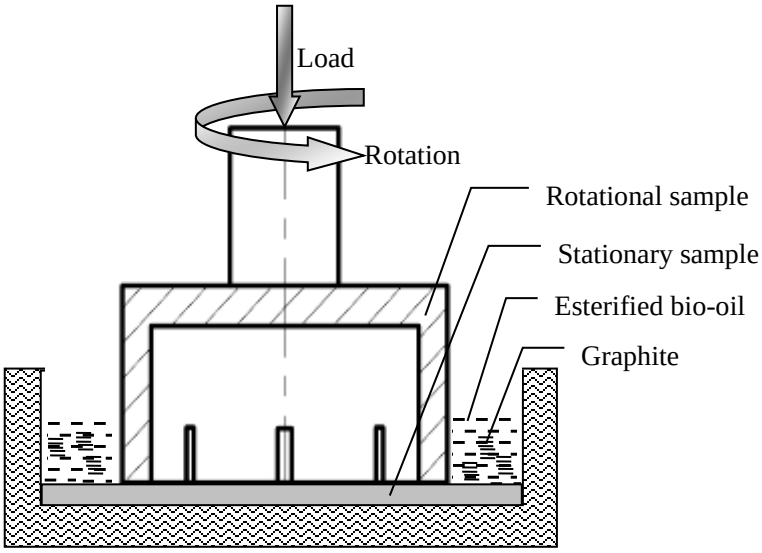

Fig.2 Illustration of the End-face tribometer

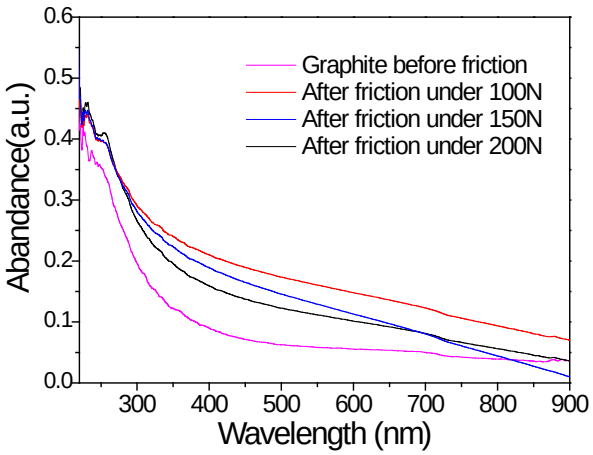

Fig.3 UV–vis spectra of graphite dispersed in EBO before and after sliding under different load

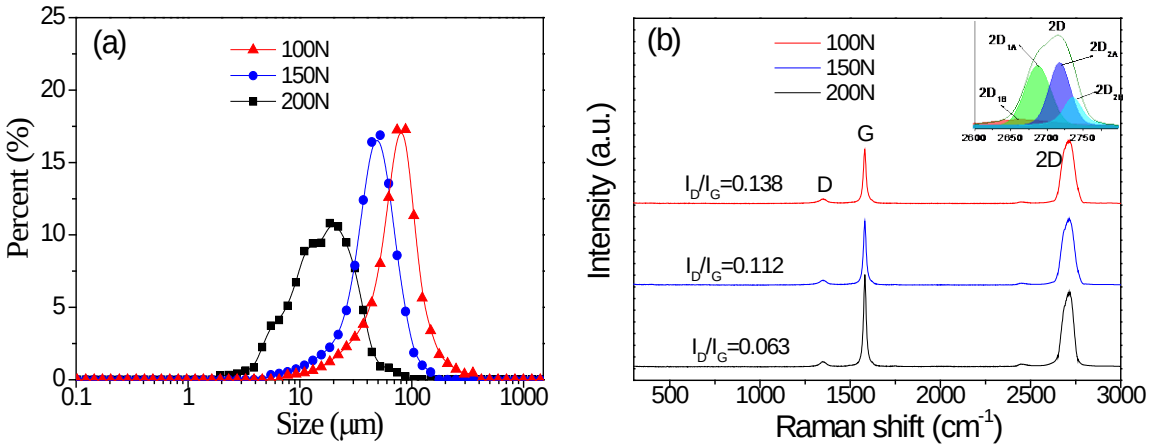

Fig.4 (a) Particle size distribution and (b) Raman spectrum of graphene transformed from graphite after sliding under different load

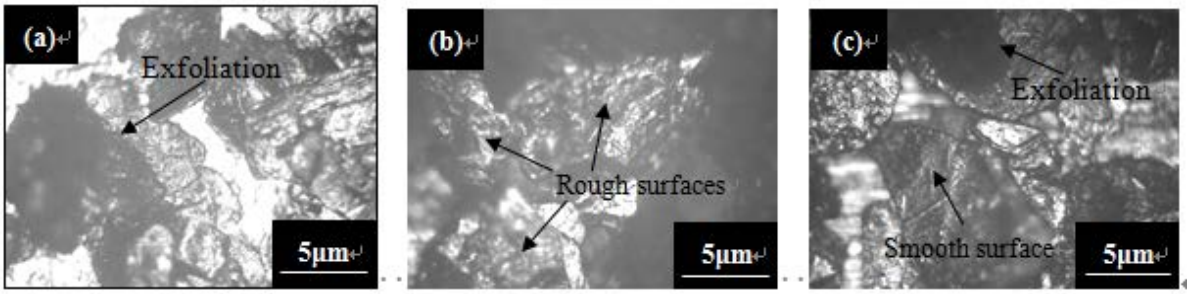

Fig.5 Micrographs of graphene transformed from graphite after sliding under different loads:

(a) 100N, (b) 150N, (c) 200N

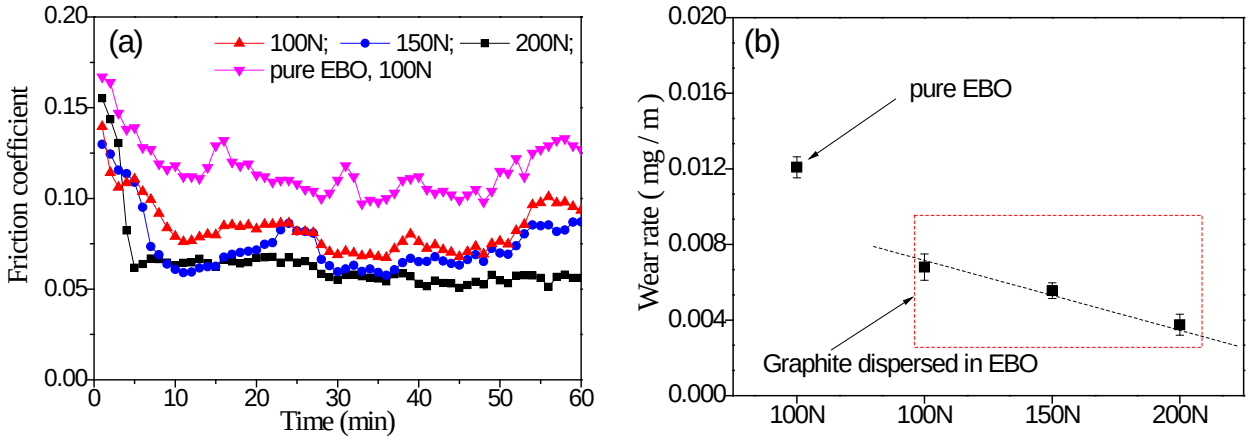

Fig.6 (a) Friction coefficient and (b) wear rate of stationary sample lubricated with EBO and graphite dispersed in EBO under different loads (sliding speed: 0.2m/s, sliding time: 60min)

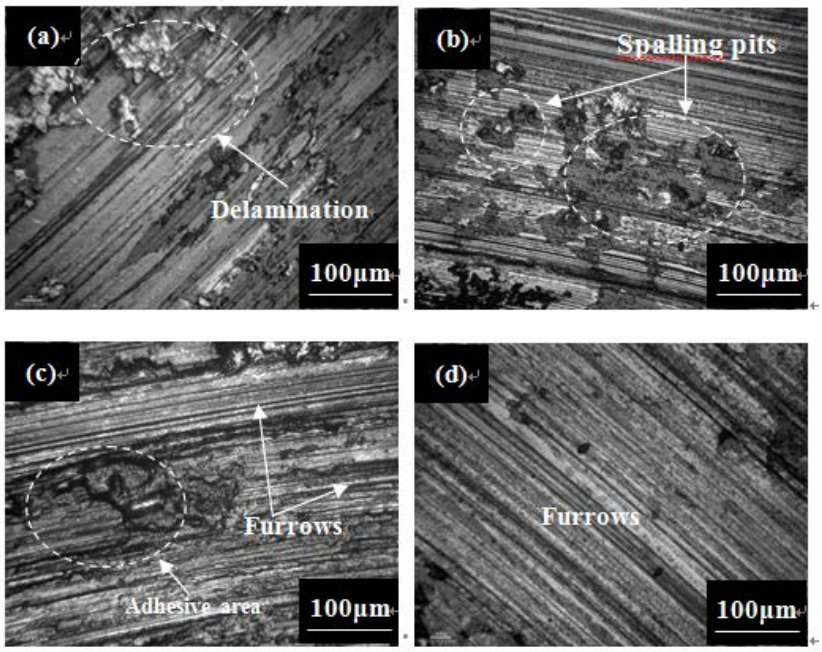

Fig.7 Micrographs of worn surfaces of stationary sample lubricated with EBO (a), and graphite dispersed in EBO under different loads: (b) 100N, (c) 150N, and (d) 200N

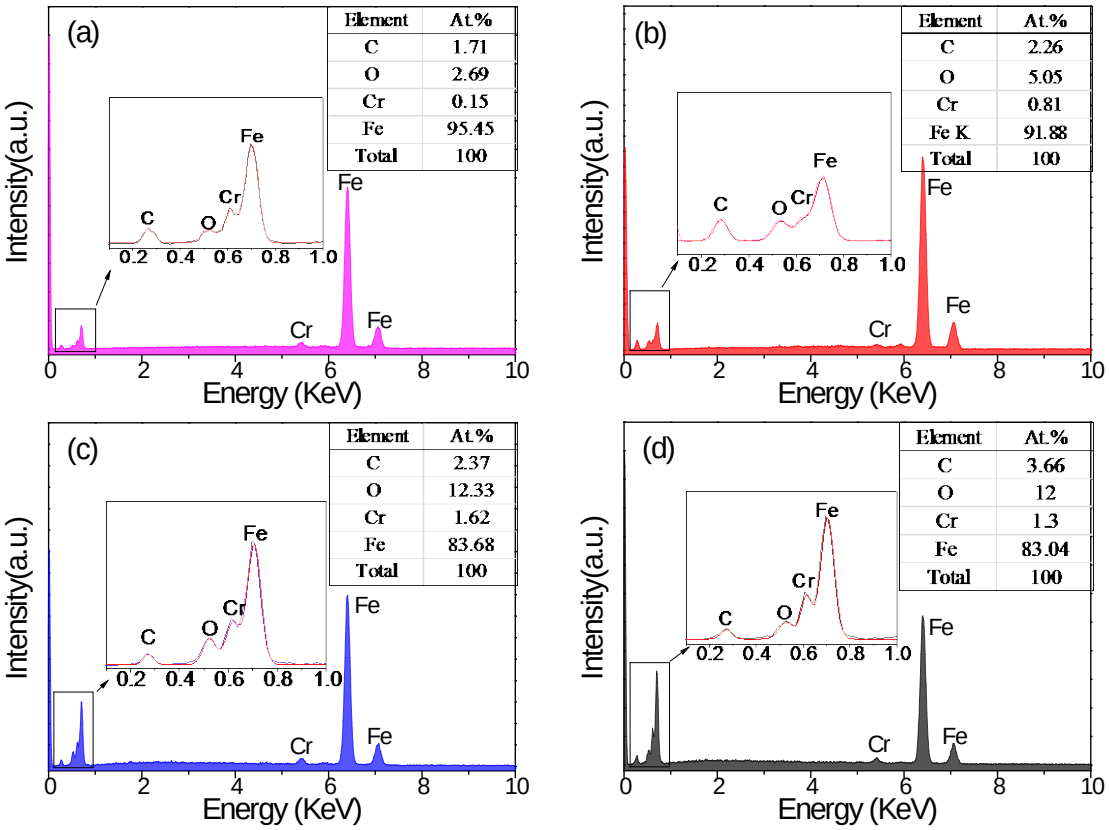

Fig.8 EDX of worn surfaces of stationary sample lubricated with EBO (a), and graphite dispersed in EBO under different loads: (b) 100N, (c) 150N, and (d) 200N

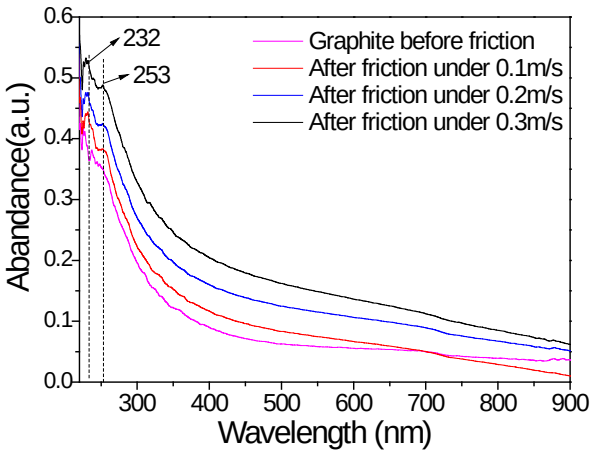

Fig.9 UV–vis spectra of graphite dispersed in EBO before and after sliding under different sliding speed (load: 250N, sliding time: 60min)

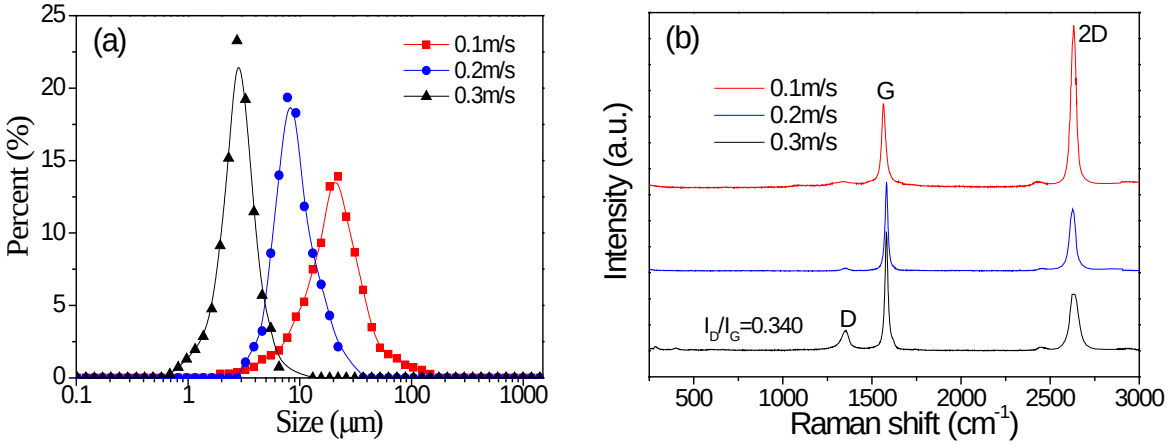

Fig.10 (a) Particle size distribution and (b) Raman spectrum of graphene transformed from graphite after sliding under different sliding speed

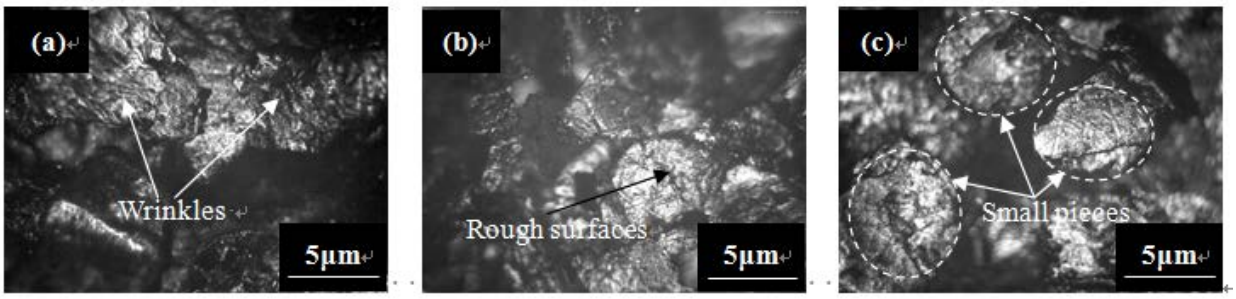

Fig.11 Micrographs of graphene transformed from graphite after sliding under different sliding speed: (a) 0.1m/s, (b) 0.2m/s, (c) 0.3m/s

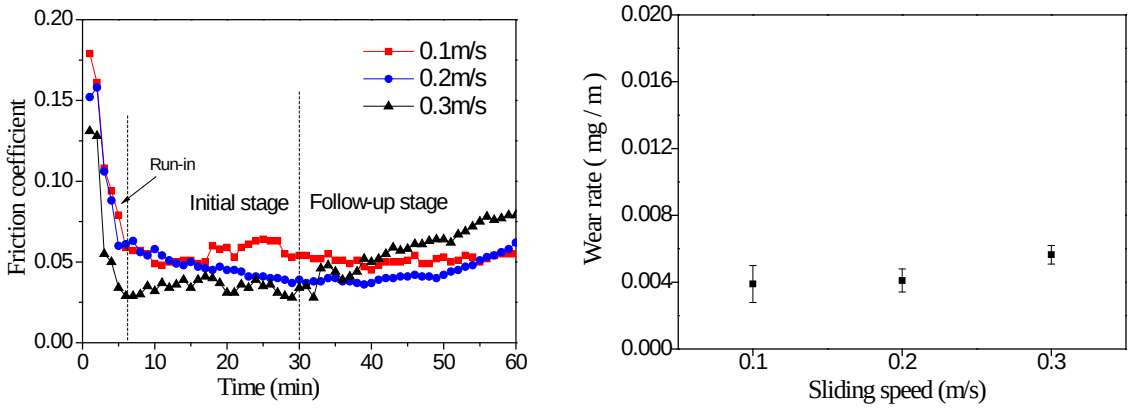

Fig.12 (a) Friction coefficient and (b) wear rate of stationary sample lubricated with graphite dispersed in EBO under different sliding speed (load: 250N, sliding time: 60min)

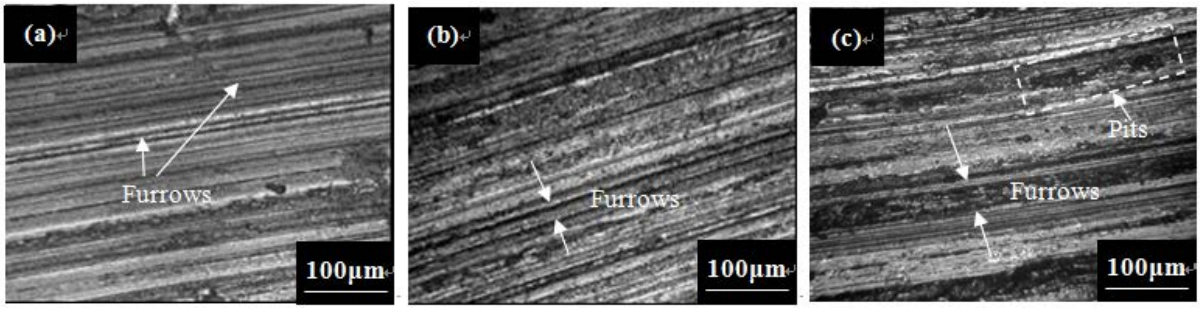

Fig.13 Micrographs of worn surfaces of stationary sample lubricated with graphite dispersed in EBO under different sliding speed: (a) 0.1m/s, (b) 0.2m/s, and (c) 0.3m/s

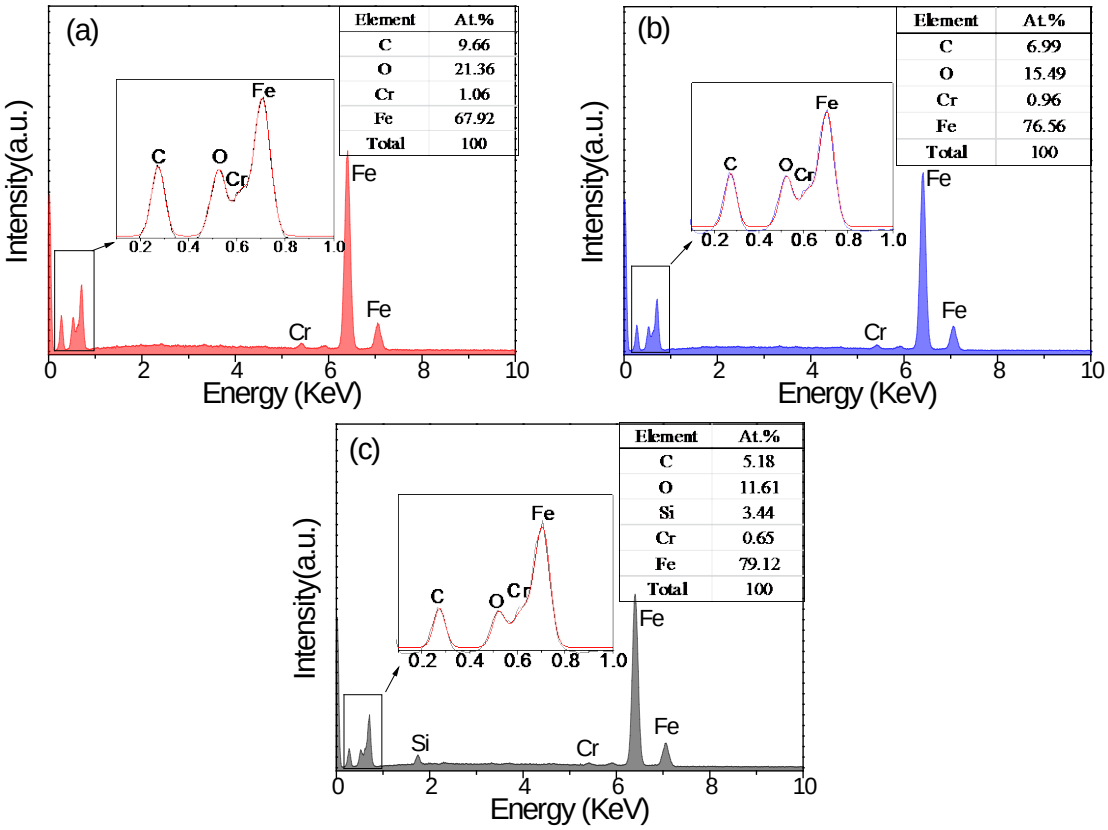

Fig.14 EDX of worn surfaces of stationary sample lubricated with graphite dispersed in EBO under different sliding speeds: (a) 0.1m/s, (b) 0.2m/s, and (c) 0.3m/s

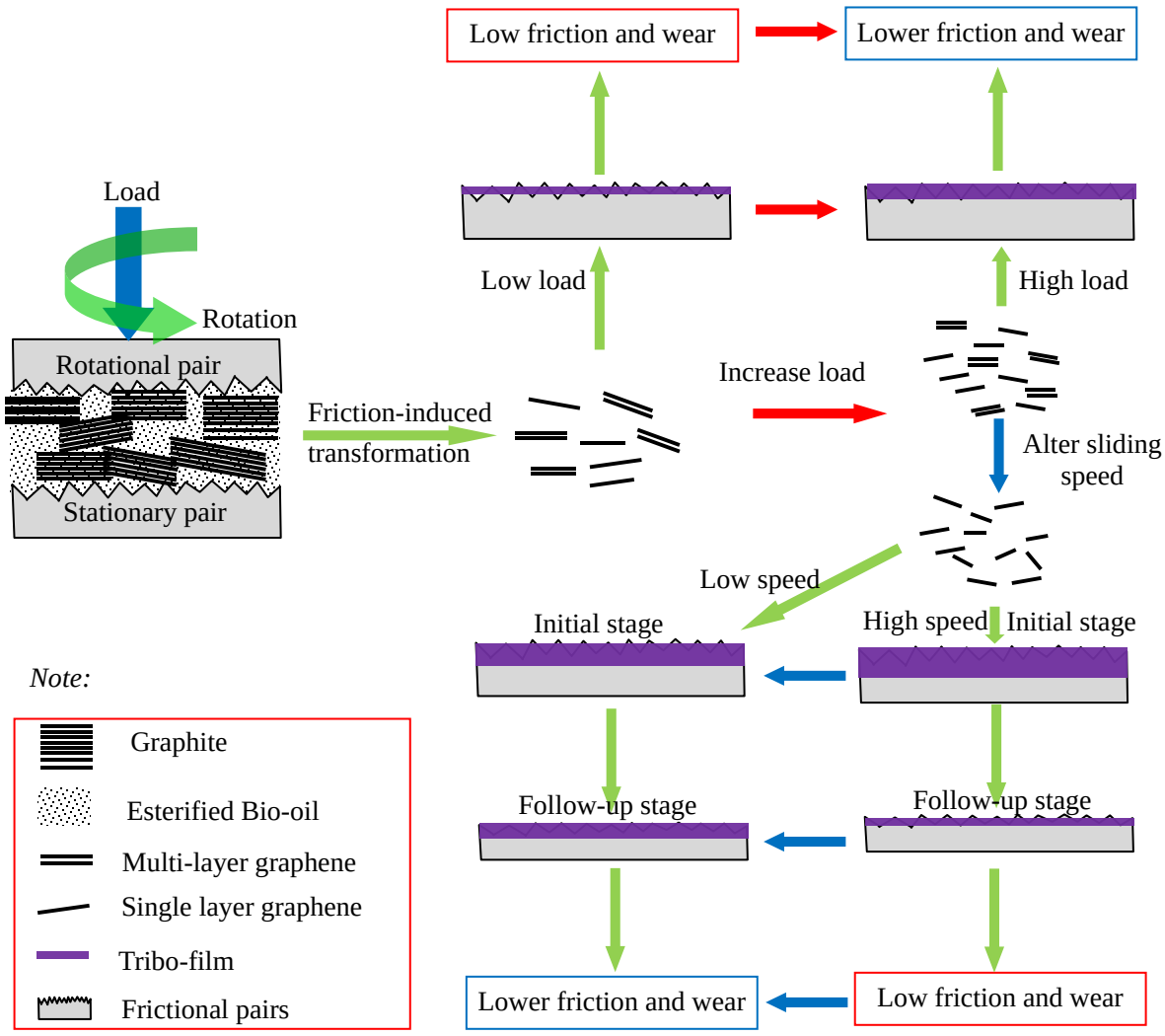

Fig. 15 Schematic explanation of tribological mechanisms